GLOBAL JOURNAL OF PURE AND APPLIED SCIENCES VOL. 8, NO. 4, SEPTEMBER 2002: 515 - 525
COPYRIGHT(C) BACHUDO SCIENCE CO. LTD. PRINTED IN NIGERIA. ISSN 1118-0579



# ROLE OF THE AMBIENT MAGNETIC FIELD *B* IN THE LONGITUDINAL VARIATION OF EQUATORIAL ELECTROJET

**C. A. ONWUMECHILI and P. O. EZEMA**

(Received 30 Januarv 2002; Revision accepted 25 April 2002)

## ABSTRACT

A review of studies of longitudinal variations of equatorial electrojet (EEJ) intensity confirms evidence of the longitudinal variation from POGO satellites data. This shows major peaks of EEJ intensity at 100°E and 190°E with a subsidiary peak at 190°E. The connection between EEJ intensity and the ambient magnetic field B has been probed with regression and power law analyses.
These reveal no statistically significant relationship between the intensity of EEJ and B, and their fittings of observations are poor. Comparison of the longitudinal profile of B along the dip equator with the average longitudinal profile of the zonal electric field $E_y$ at the dip equator proves that on the average $E_y$ is proportional to B. This conclusion also arose from the AE-E satellite observations, and therefore $E_y$ is not independent of longitude as was assumed by earlier workers. It has been suggested that Joule heating of the atmosphere which depends on the square of B produces perturbations of ionospheric drift velocity, and that the perturbations contribute to the longitudinal variation of EEJ intensity.

**Keywords:** ambient magnetic field, equatorial electrojet magnetic signature, longitudinal variation of equatorial electrojet current.

## INTRODUCTION

There was a striking difference in the reports of the longitudinal variation of equatorial electrojet (EEJ) current strength but the difference has now narrowed considerably. Using IGY data, Rastogi (1962) plotted the daily range $\Delta H$ at Huancayo, Ibadan, Jarvis, Addis Ababa, Koror and Trivandrum for December 1957, March 1958, and June 1958 on the same diagram against the ambient value of H at the stations. There was significant scatter but on the whole the impression was created that $\Delta H$ is inversely related to H. Without any quantitative analysis he concluded that $\Delta H$ varied with longitude in such a way that it decreased from Huancayo to Trivandrum in the order the stations are listed in fig. 1. Gupta (1973) plotted a similar diagram, Fig. 1, using lunar daily variation at the same stations with the addition of Kodaikanal. His Fig. 1 achieved less scatter than Rastogi's (1962).

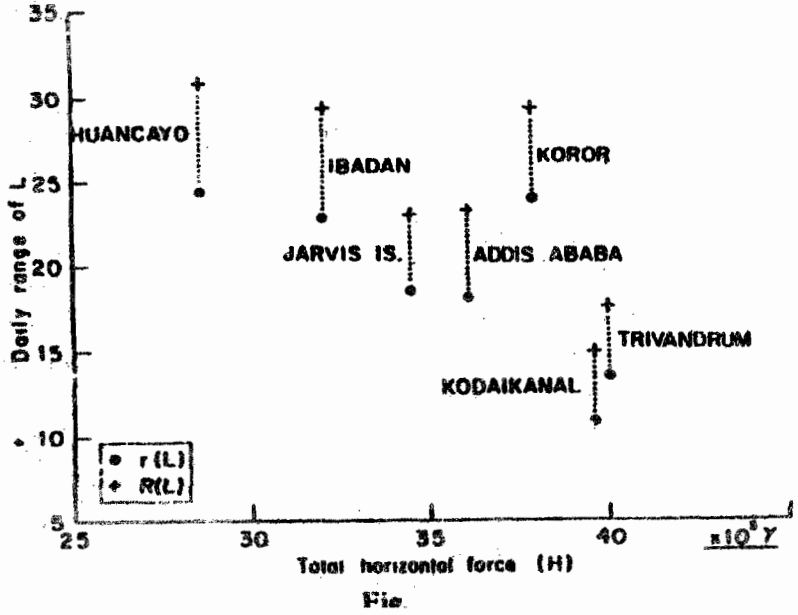


Fig. 1 The variation of the average daily range r(L) and the maximum daily range R(L) Of the geomagnetic lunar variation L in H with the magnitude of H at certain stations in equatorial electrojet zone.(After Gupta 1973)

C. A. ONWUMECHILI, Department of Physics and Astronomy, University of Nigeria, Nuskka, Nigeria
P. O. EZEMA, Department of Physics and Astronomy, University of Nigeria, Nuskka, Nigeria

One way of explaining such a relationship (i.e. achieving less scatter) is the involvement of the earth's magnetic field B in the expressions for the electrical conductivity of the ionosphere. It may be seen in Matsushita (1967) and Onwumechili (1967) that the specific conductivity of the ionosphere $\sigma$ may be expressed as

$$\sigma = {}^{1}\!/_{B} f(e, m, \omega, \nu,) \qquad 1$$

Where B is the ambient magnetic field, **e** and **m** are the charge and mass of a particle in the ionospheric plasma, and $\omega$, v are its gyro and collision frequencies respectively. However, Eq. 1 is not a simple prediction of inverse relation between $\sigma$ and B because $\omega$ is also a function of B and f is not a linear function of $\omega$. The equatorial electrojet model of Suigura and Cain (1966) was based on the eastward electrical conductivity of the ionosphere. Their conductivity, which they plotted as the equivalence of EEJ current, varied with longitude in response to B. But conductivity is not current. The equivalence can only be justified if the electric field driving the EEJ current is uniform and eastward at all longitudes, and the vertical polarization electric field completely inhibits the flow of Hall current. Furthermore, the model did not satisfy the requirement of $\nabla.j = 0$. Davis et al. (1967) produced a model of electrical conductivity similar to that of Suigura and Cain (1966).

Taking the total EEJ current above 280°E as 100 per cent, the improved EEJ model of Sugiura and Poros (1969) found that the total current at other selected longitudes were 76% at 0°E, 65% at 40°E, 56% at 80°E, and 77% at 180°E. However, since they used constant electric field $E_y$ = 2.4mV/m, this merely reflects the longitudinal variation of electrical conductivity. In effect the works of Sugiura and Cain (1966), Davis et al. (1967) and Sugiura and Poros (1969) suggest that the intensity of EEJ current varies inversely as B.

The first challenge of this view of longitudinal variation of EEJ current strength came from the observations by POGO satellites. Using the data at over 2000 traversals of the dip equator by the POGO satellites, Cain and Sweeney (1973) plotted the observed raw data of S, the magnitude of the magnetic signature of the EEJ against longitude in Fig. 2. They found substantial peaks around 100°E, 290°E and a minor peak at 195°E. Fig. 2 also shows the S at selected longitudes calculated from the theory of Davis et al. (1967) with uniform electric field. In response to the high value of B the calculated S shows a minimum at 100°E where the observed S is a maximum.

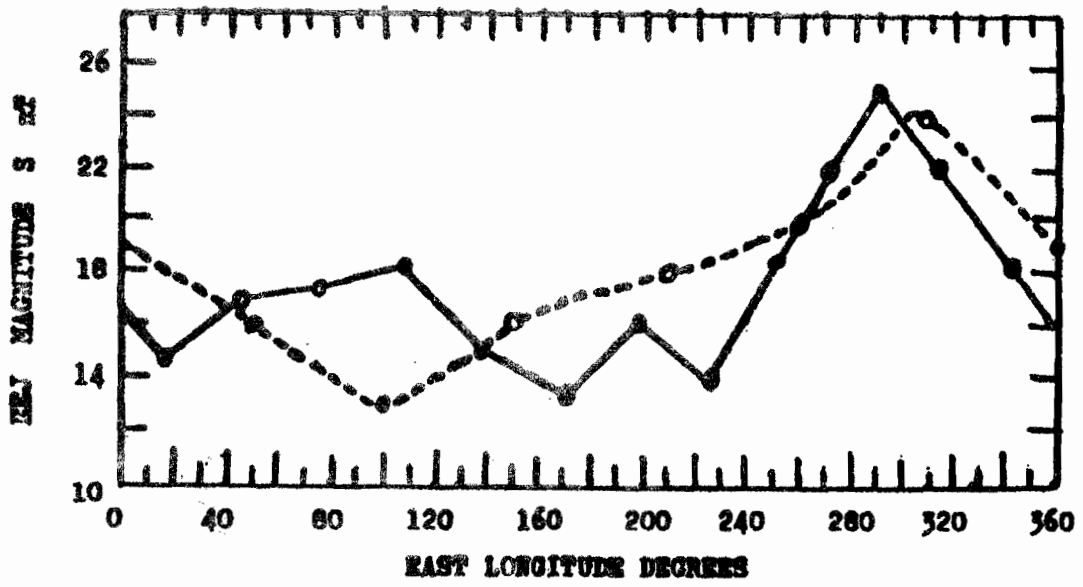


Fig. 2. Comparison of longitudinal variation of averaged magnitude S nT of the POGO equatorial electrojet magnetic signature normalized to 400km satellite altitude (solid curve) with its value calculated from the effective eastward conductivity model of Davis et al (1967) (broken curve). After Cain and Sweeney (1973), slightly modified by translating West longitude to East longitude.

The analyses of the POGO data by Onwumechili and Agu (1981), Ozoemena and Onwumechili (1987), Onwumechili et al 1989, Onwumechili and Ezema (1992), and Ezema and Onwumechili (1996) lead to the

derivation of the landmark parameters of the EEJ and its magnetic fields. From the longitudinal variation of the most comprehensive of these analyses, Ezema and Onwumechili (1996) show that the peak current density $j_o$ $Akm^{-2}$, the peak current intensity $J_o$ $Akm^{-1}$ , and the total forward current $I_F$ kA have peaks at about 100°E, 190°E, and 290°E; and troughs at about 140°E and 230°E.

On the other hand, the longitudinal variations of the percentage ratio 100Jm/Jo of the peak return current intensity $J_m$ to the peak forward current intensity Jo, the half vertical thickness p km at half of the peak current density 1/2jo, the latitudinal distance of the current focus w degree, the latitudinal distance of the peak return current intensity $x_m$ degree, and the latitudinal extent $L_1$ degree of the EEJ current from the current center show no discernible periodicities in longitude. The longitudinal variations of the earlier analyses of POGO data by Onwumechili and Agu (1981), Ozoemena and Onwumechili (1987), and Onwumechili et al (1989) are consistent with the results of Ezema and Onwumechili (1996).

Patil, Rao and Rastogi (1990) compared the strengths of the EEJ at Huancayo (285°E) and Trivandrum (77°E) during the period IQSY (International Quiet Sun Yeaars) 1964 – 1965. They found only "a marginal increase in the magnitude of the electrojet in the American over the Indian sector at local noon". They concluded that it confirmed the longitudinal variations of Onwumechili and Agu (1981) and Ozoemena and Onwumechili (1987) from the POGO data.

Onwumechili (1992ab) comprehensively compared all rocket measurements of EEJ made uo to 1973 off Peru (about 280°E) and at Thumba India (77°E). He found no significant difference not only between the current intensities but also between the vertical structural parameters of EEJ at India and Peru.

The longitudinal variation of the magnetic field of EEJ has also been given in Fig. 3 by Ravat and Hinze from Magsat satellite data. The Magsat magnetic field of EEJ is very weak because it is available for dusk and dawn only. It, therefore, had to be magnified several times for plotting. Their dusk data confirm the longitudinal variation of the $\Delta B$ of EEJ from the POGO data. The peak occurred at about 285°E with a secondary peak at about 90°E longitude. The dawn data show the opposite variation. The contrasting variations are understandable from their explanation that ionospheric currents flow eastwards at dusk but westwards at dawn. It may therefore be concluded that the Magsat data support the longitudinal variations of the POGO data.

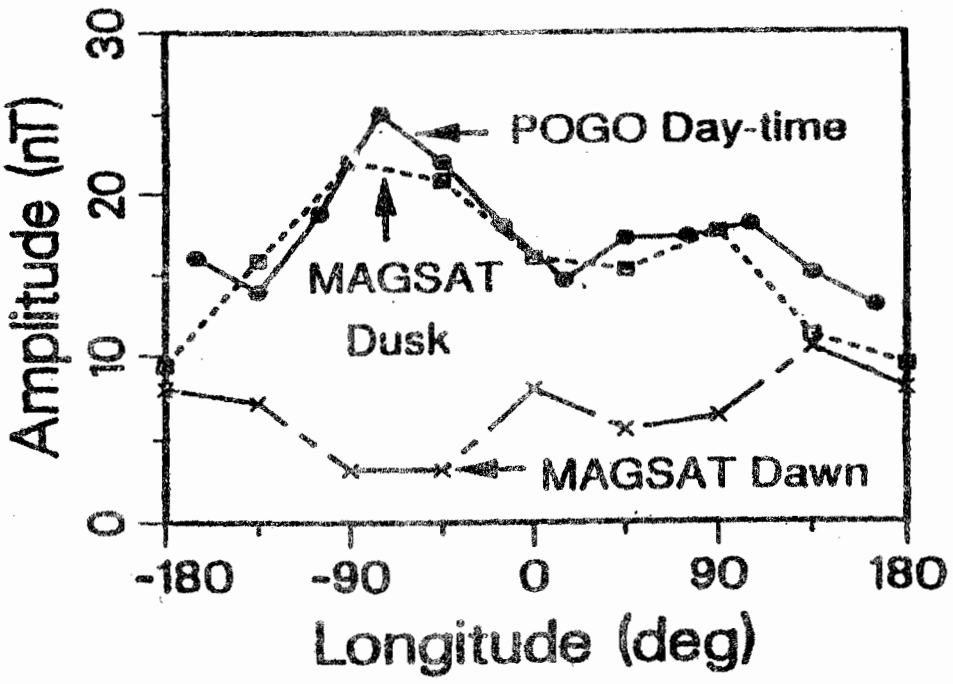


Fig. 3 Longitudinal profiles of equatorial electrojet dip-latitude average $\Delta B$ field. The POGO profile is from Cain and Sweeney (1973). Magsat dusk amplitudes are normalized to POGO amplitudes at – 90° longitude. The dawn Magsat curve is exaggerated four times its own values. After Ravat and Hinze (1993).

From the above review, it may be concluded that evidence has converged in favour of the longitudinal variation of the strength of EEJ found from the POGO data. This paper explores the functional relationship

between the ambient magnetic field B and the strength of the equatorial electrojet. It then discusses the physical mechanism likely to be responsible for the longitudinal variation of the strength of EEJ.

## CORRELATION OF GEOMAGNETIC FIELD B WITH EQUATORIAL ELECTROJET STRENGTH FROM IGY DATA

In their study of Sq during the IGY, Price and Stone (1964) calculated the dip latitudes of the stations as

$$L = \tan^{-1}(Z/2H) \qquad 2$$

For 5 stations very close to the dip equator, they gave the mean daily range $\Delta X$ of the northward magnetic field in the Lloyd seasons J, E and D. From these and their other data, we have given the annual mean $\Delta X$ in Table 1 for three groups of stations during the IGY. The (a) group of 5 stations are almost on the dip equator. The (b) group of 6 stations have dip latitudes L from $\pm 5^{\circ}$ to $\pm 10^{\circ}$ and the (c) group of nine stations have L from $\pm 10^{\circ}$ to $\pm 18^{\circ}$.

The regression analyses between $\Delta X$ and B of the stations in each group has been done. There is no appreciable tendency for $\Delta X$ to decrease as B increases within the (a) group of stations. Indeed, the calculation shows no significant negative correlation between $\Delta X$ and B. Surprisingly, there is the tendency for $\Delta X$ to increase as B increases within the (b) group of 6 and the (c) group of 9 stations in Table 1. However, calculation shows that the positive correlations found between $\Delta X$ and B in both groups are not statistically significant.

Table 1 : Annual means of daily range $\Delta$ XnT of the northward magnetic field and the earth's magnetic flux density B $\mu$ T at some low latitude stations during the IGY, taken from Price and Stone (1964). Dip latitude L = $\tan^{-1}$ (Z/2H)

| Station | North Latitude Degree | East Longitude Degree | Dip Latitude Degree | Magnetic Field B uT | Daily Range $\Delta$ X nT |
|---|---|---|---|---|---|
| | | (a) | | | |
| Huancayo | -12.03 | 284.68 | 1.0 | 28.5 | 185 |
| Jarvis | -0.38 | 199.97 | 1.1 | 34.4 | 150 |
| Addis Ababa | 9.03 | 38.77 | -0.5 | 36.0 | 147 |
| Koror | 7.33 | 134.50 | 0.0 | 37.7 | 173 |
| Trivandrum | 8.48 | 76.95 | -0.3 | 40.0 | 151 |
| | | (b) | | | |
| Tatuoca | -1.20 | 311.48 | 8.9 | 29.9 | 76 |
| M'Bour | 14.40 | 343.05 | 9.1 | 33.0 | 64 |
| Bangui | 4.60 | 18.58 | -7.0 | 33.1 | 84 |
| Fanning | 3.90 | 200.62 | 5.3 | 33.4 | 82 |
| Guam | 13.58 | 144.87 | 6.5 | 36.3 | 87 |
| Muntinlupa | 14.37 | 121.02 | 7.2 | 40.1 | 87 |
| | | (c) | | | |
| Pilar | -31.67 | 296.12 | -14.8 | 25.8 | 60 |
| Paramaribo | 5.83 | 304.78 | 17.6 | 34.3 | 64 |
| Tahiti | -17.53 | 210.42 | -15.8 | 37.8 | 66 |
| Hollanda | -2.57 | 140.2 | -10.9 | 39.8 | 94 |
| Apia | -13.80 | 188.28 | -16.3 | 40.3 | 75 |
| Alibag | 18.63 | 72.87 | 12.9 | 42.4 | 73 |
| Port Moresby | -9.40 | 147.15 | -17.6 | 42.9 | 69 |
| Djakarta | -6.03 | 106.73 | -17.6 | 44.2 | 77 |
| Chapa | 22.35 | 103.83 | 15.8 | 44.8 | 63 |

It is believed that in the narrow ranges of L within each of the 3 groups, the small differences in L cannot be responsible for the results. Therefore, the analysis does not support the expectations from Rastogi (1962), Gupta (1973), Sugiura and Cain(1966) and Sugiura and Poros (1969).

## TESTING A POWER LAW RELATION BETWEEN B AND EQUATORIAL ELECTROJET STRENGTH INDICATORS

It has already been mentioned that despite Eq. 1, the specific conductivities $\sigma$ are not simple functions of the gyrofrequency $\omega$ = eB/m nor of B. The layer conductivities, which directly support current flow, are even more complicated functions of $\omega$ and B. Nevertheless, the factor 1/B in Eq. 1 suggests the investigation of a power law relationship of the type

$$j_o = cB^m \qquad 3$$

where c and m are constants and $j_o Akm^{-2}$ is the peak current density of the equatorial electrojet (EEJ). Since $\Delta X$ is an indicator of the strength of ionospheric current, it could replace $j_o$ in Eq. 3

The analyses of Ezema and Onwumechili (1996) have the annual means of $j_o$ for local time hours 09 hr to 15 hr and for the all daytime averages for the years 1968, 1969 and for 1967 – 1969 at intervals of 10° longitude. The International Geomagnetic Reference Field (IGRF) has been used to calculate the values of B at the dip equator in 1968 and 1969 at 10° intervals of longitude corresponding to the annual mean peak

Table 2 Daytime peak current density $j_o Akm^{-2}$ of the equatorial electrojet and the geomagnetic field B in 1968 and 1969 at intervals of longitude along the magnetic dip equator. After Onwumechili 1997.

| 1968 | | | | | 1969 | |
|---|---|---|---|---|---|---|
| Magnetic Field B NT | Current Density $Akm^{-2}$ | North Latitude Degree | East Longitude Degree | North Latitude Degree | Magnetic Field B nT | Current Density $Akm^{-2}$ |
| 32389 | 7.4 | 10.13 | 0 | 10.17 | 32411 | 3.8 |
| 33422 | 6.4 | 10.40 | 10 | 10.42 | 33445 | 3.6 |
| 34441 | 6.0 | 10.36 | 20 | 10.40 | 34465 | 3.8 |
| 35307 | 6.6 | 10.08 | 30 | 10.08 | 35316 | 3.8 |
| 35958 | 7.0 | 9.36 | 40 | 9.36 | 35957 | 3.9 |
| 36645 | 7.2 | 8.56 | 50 | 8.59 | 36634 | 3.9 |
| 37687 | 6.8 | 8.20 | 60 | 8.20 | 37669 | 4.6 |
| 39032 | 7.9 | 8.50 | 70 | 8.52 | 39016 | 7.0 |
| 40254 | 10.0 | 9.13 | 80 | 9.16 | 40241 | 9.5 |
| 40969 | 11.7 | 9.52 | 90 | 9.52 | 40956 | 11.6 |
| 41028 | 12.1 | 9.33 | 100 | 9.33 | 41021 | 12.7 |
| 40514 | 10.4 | 8.74 | 110 | 8.74 | 40511 | 10.9 |
| 39620 | 8.0 | 8.17 | 120 | 8.17 | 39620 | 8.3 |
| 38476 | 5.0 | 7.86 | 130 | 7.86 | 38475 | 5.2 |
| 37159 | 4.2 | 7.67 | 140 | 7.7 | 37150 | 4.4 |
| 35857 | 4.5 | 7.30 | 150 | 7.35 | 35842 | 4.7 |
| 34900 | 7.0 | 6.30 | 160 | 6.35 | 34882 | 6.8 |
| 34479 | 10.0 | 4.50 | 170 | 4.50 | 34471 | 9.4 |
| 34435 | 12.0 | 2.05 | 180 | 2.29 | 34368 | 10.9 |
| 34201 | 12.8 | 0.35 | 190 | 0.38 | 34173 | 10.4 |
| 33782 | 10.9 | -0.90 | 200 | 0.90 | 33753 | 7.7 |
| 33272 | 9.0 | -1.80 | 210 | 1.81 | 33242 | 5.8 |
| 32776 | 6.9 | -2.62 | 220 | 2.65 | 32743 | 4.3 |
| 32311 | 5.7 | -3.50 | 230 | 3.50 | 32274 | 6.0 |
| 31886 | 5.4 | 4.35 | 240 | 4.35 | 31846 | 7.1 |
| 31456 | 5.9 | 5.45 | 250 | 5.47 | 31410 | 9.3 |
| 30838 | 7.0 | 8.15 | 260 | 7.16 | 30786 | 10.2 |
| 29822 | 10.2 | 9.50 | 270 | 9.53 | 29759 | 12.5 |
| 28382 | 12.2 | 12.05 | 280 | 12.05 | 28318 | 13.2 |
| 26868 | 14.8 | 13.78 | 290 | 13.74 | 26811 | 13.6 |
| 25962 | 14.5 | 13.39 | 300 | 13.33 | 25911 | 10.6 |
| 26092 | 13.5 | 10.29 | 310 | 10.17 | 26062 | 9.5 |
| 27117 | 10.7 | 4.89 | 320 | 4.72 | 27112 | 7.6 |
| 28633 | 7.7 | 1.37 | 330 | 1.53 | 28639 | 7.6 |
| 30121 | 7.1 | 6.29 | 340 | 6.43 | 30139 | 5.6 |
| 31345 | 6.9 | 9.04 | 350 | 9.13 | 31367 | 4.5 |
| 33818 | 8.6 | | Mean | | 33800 | 7.6 |
| 4311 | 2.9 | | SD | | 4320 | 3.3 |

current densities $j_o$. Table 2 gives an example of these for 1968 and 1969. The corresponding values of $\Delta X$ and B are also available in Table 1 for the longitudes of the IGY stations.

Taking the logarithms of the power law produces a linear relationship. The least square fitting of the power law then gives the value of the exponent m. The values of m obtained from three sets of $j_o$ and B, and three sets of $\Delta X$ and B are given in the following table.

| Parameter Pairs | Exponent m | Parameter Pairs | Exponent m |
|---|---|---|---|
| 1968 $j_o$ vs 1968 B | - 0.7 | IGY (a) group $\Delta X$ vs B | - 0.5 |
| 1969 $j_o$ vs 1969 B | - 0.6 | IGY (b) group $\Delta X$ vs B | - 0.55 |
| 1967 - 69 $j_o$ vs 1968 B | - 0.6 | IGY (c) group $\Delta X$ vs B | - 0.35 |

For the equatorial electrojet zone the value of m is consistently about –0.6. However, the 6 values of the exponent m only –0.7 is significant at 5 percent and the rest are not statistically significant at that level. The positive values of the exponent m are surprising. It is difficult to understand why the strength of one part of the Sq current system should decrease with the magnitude of B while the strength of other part of Sq current system increases with the magnitude of B. The lack of statistical significance at 5 percent level may be important. However, the conclusion from this test is that the strength of the equatorial electrojet tends to decrease as $B^m$ where $m \approx -0.6 \pm 0.08$, while the strength of the world-wide part of Sq appears to increase weakly as B increases.

Fig. 4 compares the longitudinal variation of B in 1968 as in Fig. 4c, with the longitudinal variation of $j_o$ in 1968 as in Fig. 4b, in 1969 as in Fig.4a, in 1967 – 1969 as in Fig. 4d (solid curve), and also with the peak return current density $j_m$ $Akm^{-2}$ in 1967 – 1969 as in Fig. 4e.While $j_o$ has peaks at about 100°E, 190°E and 290°E with troughs around 140°E and 230°E, the peaks and troughs of $J_m$ are the reverse. The variations of the current densities show no obvious relationship with B. In particular, both the peak and the trough of B correspond to the peaks of the current $j_o$.

In the panel for Fig. 4 (d): the solid curve is the observed $j_o$ for 1967 – 1969, the broken curve is the $j_o$ calculated from the power law Eq. 3 for 1967-1969, and the dotted curves demarcate the variance limits of the observed $j_o$. Although the observed $j_o$ remains mostly within the variance limits of the observed jo, the fitting of the pwer law is not good. (i) The mean residual is larger than the mean value. (ii) The calculated trend is opposite the observed trend around 100°E longitude. On the whole the power law relation is unsatisfactory.

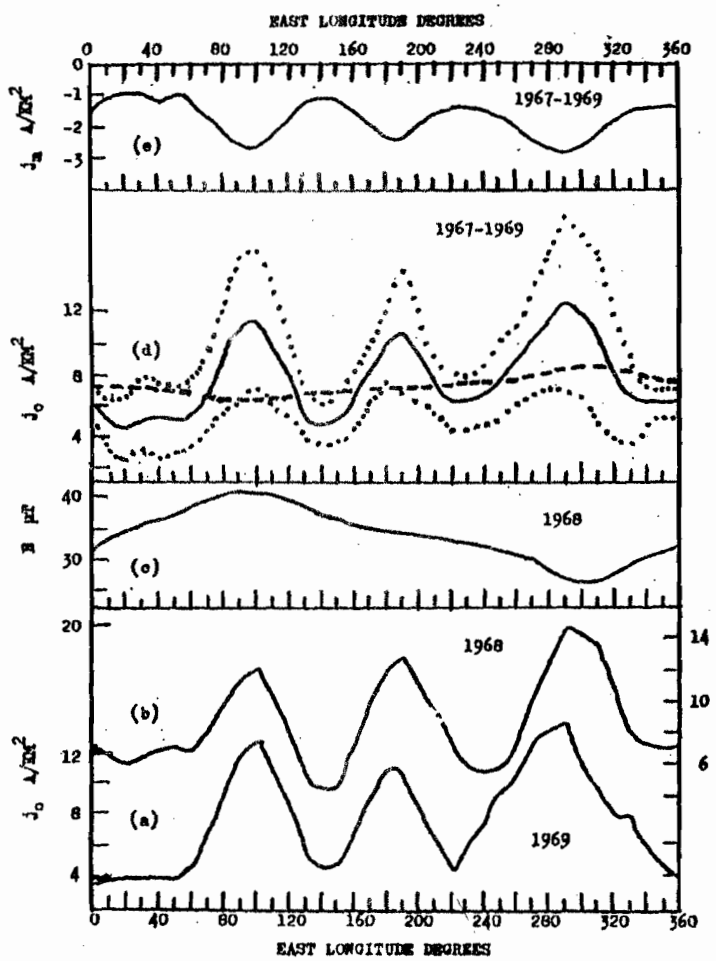


Fig. 4 Comparison of the longitudinal variation of (c) the geomagnetic field intensity B μT with the peak equatorial electrojet current density $j_o$ A/km$^2$ (a) for 1969, (b) for 1968, (d) solid curve for 1967 – 1969 and (e) with the peak westward return current density $j_m$ A/km$^2$. In (d) the dotted curves demarcate the variance limits and the broken curve is the calculated $j_o$ from the power law, $j_o = cB^m$ with $m = -0.59$. After Onwumechili 1997.

## SATELLITE INVESTIGATIONS OF LONGITUDINAL VARIATIONS OF ELECTRIC FIELD AND EQUATORIAL ELECTROJET CURRENT

Coley, McClure and Hanson (1990) used the very large data on ion drift for 1977- 1979 measured by the Atmospheric Explorer E, (AE-E) satellite in the dip equatorial region to investigate the longitudinal variation of the vertical drift velocity $V_z$. They first demonstrated that their diurnal profile of $V_z$ for the location of Jicamarca agrees very well with incoherent radar observations at Jicamarca, and is consistent with the empirical global model of Richmond et al. (1980).

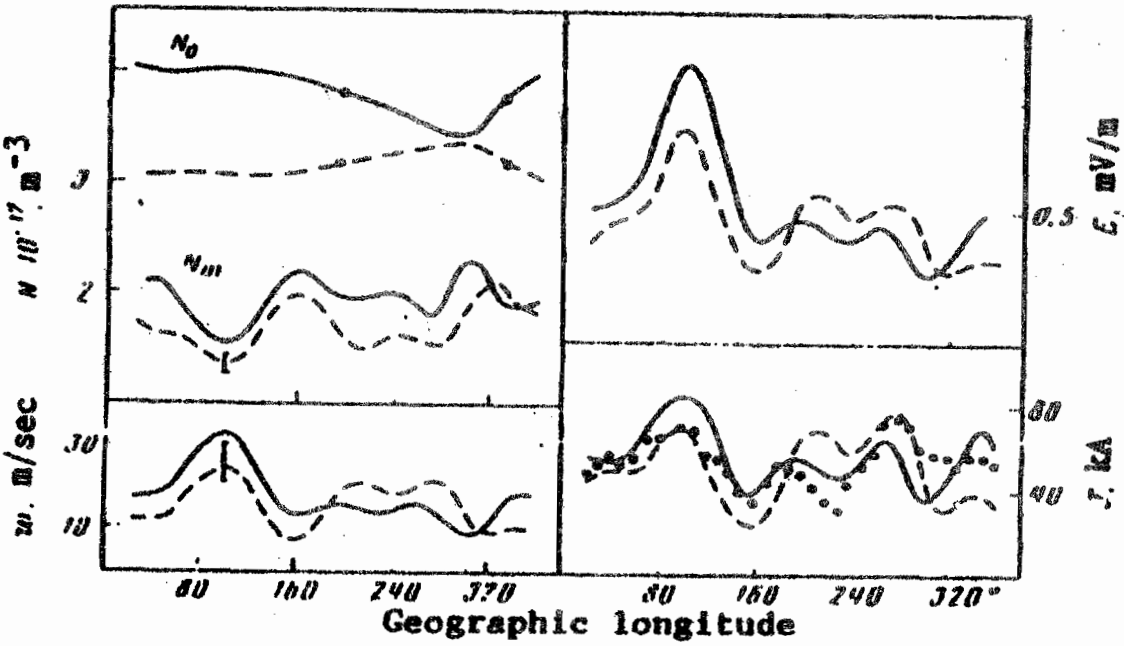


Fig. 5 Longitudinal variations of the electron concentration of the maximum of the F2 layer $N_m$ according to data of the IK.19 satellite, the vertical projection of the drift velocity $\omega$, the zonal component of the electric field E, and the total current of the equatorial electrojet I, near 14 hr L.T. In December (solid curve) and June (dashed curve) 1980. The filled circles denote the data from Leshchinskaya et al (1985), and $N_o = N_m$ at $\omega = 0$. After Deminov et al (1988).

They then investigated the vertical ion drift $V_z$ in the two longitude sectors: a 135° sector from –130°E to 5°E centered on the minimum value of B (297.5°E) near Jicamarca, and a 100° sector from 60°E to 160°E centered on the maximum value of B (110°E) near Malaysia. Using the data of 1978 – 1979 they compared the values of $V_z$ in the low-B and high-B sectors within the zone of –10° dip latitude to 10° dip latitude. They found that the average magnitude of the vertical drift $V_z$ over 24 hours of local time was 13.4 m/s (from 18,914 data points) for the low-B region and 15.3 m/s (from 10,012 data points) for the high-B region.

They considered that the difference in $V_z$ in the low-B and high-B regions is too small. Because $V_z = E_y/B$ the difference also has the wrong sign if the zonal dynamo electric field $E_y$ had been independent of longitude as assumed by Sugiura and Cain (1966), and Sugiura and Poros (1969). They concluded that on the contrary, on the average, $V_z$ is independent of longitude and $E_y$ is proportional tc B. The Sq dynamo action ties $E_y$ to the emf $\underline{W} \times \underline{B}$ induced by the ionospheric plasma carried in the neutral wind $\underline{W}$. Expecting $\underline{W}$ to be on the average independent of longitude, Richmond et al. (1980) had assumed the above conclusion of Coley et al. (1990).

Deminov, Kochenova and Sitnov (1988) used the data of Interkosmos 19 (IK-19) satellite for June and December 1980 to investigate the longitudinal variations of the Sq dynamo zonal electric field $E_y$ and the total EEJ forward current at 14 hr local time in the EEJ zone. Fig. 5 gives their results. Their longitudinal variations of EEJ total forward current in June and December on the bottom right panel have all the essential features of the longitudinal variations of the peak current density jo in Fig. 4. Indeed, their longitudinal variation of EEJ total current from the data of Leshchinskaya et al. (1985), shown by the dotted curve is almost a faithful reproduction of the variation of $j_o$ in Fig.4.

On the top right curve of Fig. 6 Deminov et al. (1988) give the longitudinal variation of the 100°-sesctor

moving average of the zonal electric field $E_y$, here denoted by $E_c$ (solid curve), and its determination from inversion theory (dotted curve). Their purpose is to establish a steady background level on which perturbations are superposed to produce the variations in Fig. 5. Comparison shows that these average curves for $E_y$ on the top right of Fig. 6 are proportional to the curve for B in Fig. 4c. This proves that on the average, the zonal electric field $E_y$ is proportional to the ambient magnetic field B as was later concluded by Coley et al. (1990). However, this important conclusion was not articulated by Deminov et al (1988).

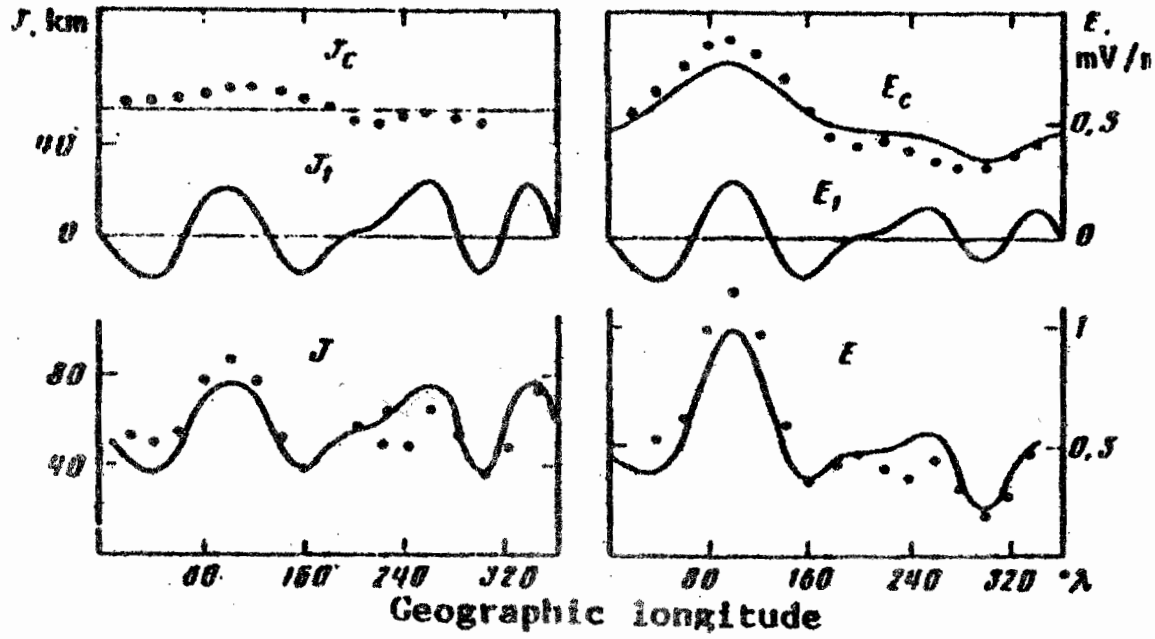


Fig.6 Longitudinal variations of the electric field and total current of the EEJ in the Zeroth ($I_c$, $E_c$) and first ($I_1$, $E_1$) approximations. $E = E_c + E_1$, $I = I_c + I_1$, near 14 hr L.T. in December. The filled circles depict the solution of the inverse problem and the solid curves depict theory. After Deminov et al (1988).

## PHYSICAL MECHANISM FOR THE LONGITUDINAL VARIATION OF EQUATORIAL ELECTROJET CURRENT

Deminov et al. (1988) believe that Joule heating of the atmosphere is responsible for the perturbation of the background levels of the zonal electrojet field $E_y$ and the total EEJ forward current $I_F$ here denoted by I. They attribute the longitudinal variations to the perturbations. They propose that the heating rate Q is proportional to the square of B. From this they calculated the first order perturbations $E_1$ and $I_1$ in Fig. 6. The perturbations are superposed on the background $E_c$ and $I_c$ to produce the observable E and I on the bottom

panels of Fig.6. These E and I variations have the general features of the right panel of Fig.5 and of Jo in Fig.4 but lack some of their significant details. A significant blemish is the minimum at 300°E which is so close to the POGO maximum at 290°E.

We prefer to consider the Joule heating proposal as follows. The heating rate

$$Q = J^2/\sum_3 = E^2 \sum_3 \propto B^2 \sum_3 \qquad 4$$

Where $\sum_3$ is the height-integrated Cowling conductivity, E is the electric field, and B is the magnetic field. The proportionality of the last two terms takes into account the proportionality of E to B found in section 4 above.

Thus the conductivity in Eq 4 moderates the dependence of Q on $B^2$.In particular, the maximum conductivity at about 300°E compensates for the low B there.This might remove or minimize the false minimum of J shown by Deminov et al. (1988) at 300°E in Fig.6. Deminov et al. (1988) believe that the Joule heating increases the drift velocity and therefore the current. The increased current in turn increases the heating rate and the cycle continues until the drift velocity reaches the critical velocity equal to the ion acoustic velocity. Then the two stream plasma instability ensues and creates EEJ electron density irregularities as discussed in Fejer and Kelley (1960).

It is possible that the Joule heating accounts for the small difference in the diurnal profiles of $V_z$ for the low B and high B regions in Fig.7 from Coley et al. (1990)

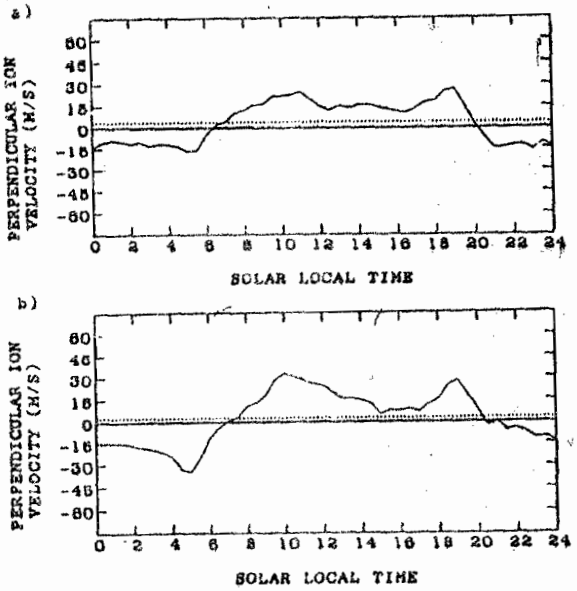


Fig.7 (a) Average diurnal curve of perpendicular ion velocity for low – B longitude region (-130°E to 5°E longitude).
(b) Average diurnal curve of perpendicular ion velocity for high – B longitude region (60°E to 160°E longitude). After Coley et al (1990).

The important conclusion that $E_y$ is proportional to B makes the current intensity of EEJ

$$J = E_y \sum_3 \propto B \sum_3 \qquad 5$$

Although $E_y$ and $\sum_3$ may not contribute equally to J, Eq.5 helps to understand the longitudinal variation of EEJ current. The maximum B at 100°E accounts for the peak current there while the maximum conductivity at 290°E accounts for the peak current there. A suitable combination of substantial magnitudes of B and $\sum_3$ at 190°E may also account for the subsidiary current peak there. Detailed calculation will be needed to test several ideas and suggestions in this section.

## CONCLUSIONS

From 1962 to 1972 it was believed that the intensity of the equatorial electrojet (EEJ) was a minimum around 100°E and a maximum around 290°E. It was thought that driving electric field $E_y$ was independent of longitude and that the intensity followed longitudinal variation of conductivity which was adjudged inversely proportional to the ambient magnetic field B.

2 The observations of POGO satellites covering all longitudes found major maxima of EEJ intensity around 100°E and 290°E, and a subsidiary maximum around 190°E. This has now been confirmed by comprehensive analyses of POGO data, by Magsat satellites data, by comparison of daily range of H around 80°E and 285°E, and by comparison of rocket measurements of EEJ around 80°E and 280°E.

3 Regression analysis finds no statistically significant inverse relationship between the intensity of EEJ and the ambient magnetic field B.

4 Fitting the intensity of EEJ to $B^m$ leads to the exponent m = -0.6 $\pm$ 0.08. This is not statistically significant, and the fitting of the observed and calculated values is rather poor.

5 The regression and power law analysis produced a surprise. While the intensity of EEJ tends to decrease weakly with increase in the magnitude of B, the intensity of the worldwide part of Sq outside but close to EEJ zone tends to increase weakly with increase in B but none was statistically significant.

6 Observations of ion drift velocity by AE-E satellite has led to the conclusion that on the average the

zonal electric field $E_y$ driving the EEJ is proportional to the ambient magnetic field B. The $E_y$ is not independent of longitude as was assumed by earlier workers.

7 Comparison of the longitudinal profile of B along the dip equator calculated from IGRF with the average longitudinal profile of zonal electric field $E_y$ driving EEJ derived from 1k – 19 satellite observations proves that on the average $E_y$ is proportional to B

8 Calculations of Deminov et al. (1988) from the observation of Ik-19 and other Russian satellites produce longitudinal variations of EEJ current with three peaks very similar to those from the POGO satellites observations.

9. It has been suggested that Joule heating of the atmosphere which depends on the square of B produces perturbations of ionospheric drift velocity, and that the perturbations contribute to the longitudinal variation of EEJ intensity.

**REFERENCES**

Cain, J. C. and Sweeney, R. E., 1973. The POGO Data, J. Atmos. Terr. Phys. 35: 1231 – 1247.

Coley, W. R., McClure J. P., and Hanson, W. B., 1990. Equatorial fountain effect and dynamo drift signatures from AE-E observations, J. Goephys. Res., 95: 21285 –21290

Davis, T. N., Burrows K., and Stolarik, J.D., 1967. A latitude survey of the equatorial electrojet with rocket-borne magnetometers, J.Geophys. Res., 72: 1845- 1861.

Deminov, M. G., Kochenova, N. A., and Yu. S. Sitnov, 1988. Longitudinal variations of the electric field in the dayside equatorial ionosphere, Geomagnetism and Aeronomy, 28: 57-60. (English translation).

Ezema, P. O., Onwumechili, C. A. and Oko, S. O., 1996. Geomagnetically quiet day ionospheric currents over the Indian Sector – III.Counter equatorial electrojet currents. J.Atmos. Terr. Phys., 58(5): 565-577.

Fejer, B. G. and Kelly, M. C ., 1980. Ionospheric Irregularities. Rev. Geophys. Space. Phys., 18: 401-454.

Gupta J.C., 1973. On solar and lunar equatorial electrojets, Ann. Geophys., 29: 49-60.

Leschinskaya, T. Yu and Mikhaylov, A. B., 1985. Yearly variation of the parameters of the daytime F2 layer near the geomagnetic equator, Geomagnetism and Aeronomy, 25: 32-35. (English translation).

Matsushita, S., 1967. Solar quiet and lunar daily variation fields, Chapter III-I in Physics of Geomagnetic Phenomena, edited by Matsushita S. and W.H. Campbell, Academic Press, New York, 1: 301-424.

Onwumechili, C .A., 1967. Geomagnetic variations in the equatorial zone, Chapter III-2 in Physics of Geomagnetic Phenomena, edited by Matsushita S. and W.H. Campbell, Academic Press., New York, 1: 425-507.

Onwumechili, C. A., 1992a. A study of rocket measurements of ionospheric currents at – III: ionospheric currents the magnetic dip equator, Geophysics, J. Int., 108: 647-659.

Onwumechili, C. A., 1992b. A study of rocket measurements of ionospheric current – V. Modelling rocket profiles of low-latitude Ionospheric currents, Geophys. J. Int., 108: 673-682.

Onwumechili, C. A., 1997. The Equatorial Electrojet. Gordon and Breach Publishers.

Onwumechili, C. A., and C.E. Agu, 1981. Longitudinal variation of equatorial electrojet parameters derived from POGO satellite observations, Planet Space. Sci., 29: 627-634.

Onwumechili, C. A., and Ezema, P. O., 1992. Latitudinal and Vertical parameters of the equatorial electrojet from an autonomous data set J.Atmos. Terr. Phys., 54: 1535 – 1544.

Onwumechili, C. A.; Ozoemena P. C., and Agu, C. E., 1989. Landmark values of equatorial electrojet current and magnetic field along a meridian near noon. Geomag. Geoelectric, 41: 443- 459.

Ozoemena, P. C. and Onwumechili, C. A., 1987. Global variations of the POGO electrojet parameters during the solstices, J.G. Geomag. Geoelectr., 39: 625-636.

Patil, A. R.; Rao D. R. K and Rastogi, R. G., 1990. Equatorial electrojet strengths in the Indian and American sectors –I. During low solar activity, J. Geomag. Geoelectr. 42: 801-811.

Price, A. T. and Stone, D. J., 1964. The quiet-day geomagnetic variations during the IGY, Annals of IGY, 35: 62-274. Pergamon Press Oxford.

Rastogi, R. G., 1962. Longitudinal variation in the equatorial electrojet, J,Atmos. Terr. Phys., 24: 1031-1040.

Ravat, D and Hinze, W. J., 1993. Considerations of variation in ionospheric field effects in mapping equatorial lithospheric Magsat magnetic anomalies, Geophys. J. Int., 113: 387-398.

Richmond, A. D.; Blanc, M.; Emery, R. H.; Wand, B.; Fejer, B. G.; Woodman, R. F.; Ganguly, S.; Amayene, P.; Behnke R. A.; Calderon, C., and Evans, J. V., 1980. An empirical model of quiet day ionospheric electric fields at middle and low latitudes, J. Geophys., Res., 85: 4664-4685.

Sugiura, M. and Cain, J. C., 1966. A model equatorial electrpjet, J. Geophys. Res., 71: 1869 – 1877.

Sugiura, M. and Poros, D. J., 1969. An improved model equatorial electrpjet with a meridional current system, J. Geophys. Res., 74: 4025 – 4034.